

UCSF

UC San Francisco Previously Published Works

Title

Hedgehog pathway mutations drive oncogenic transformation in high-risk T-cell acute lymphoblastic leukemia.

Permalink

<https://escholarship.org/uc/item/02f9n3q6>

Journal

Leukemia, 32(10)

ISSN

0887-6924

Authors

Burns, Melissa A
Liao, Zi Wei
Yamagata, Natsuko
et al.

Publication Date

2018-10-01

DOI

10.1038/s41375-018-0097-x

Peer reviewed



Published in final edited form as:

Leukemia. 2018 October ; 32(10): 2126–2137. doi:10.1038/s41375-018-0097-x.

Hedgehog pathway mutations drive oncogenic transformation in high-risk T-cell acute lymphoblastic leukemia

Melissa A. Burns^{1,2}, Zi Wei Liao¹, Natsuko Yamagata¹, Gayle P. Pouliot^{1,2}, Kristen E. Stevenson³, Donna S. Neuberg³, Aaron R. Thorner⁴, Matthew Ducar⁴, Emily A. Silverman¹, Stephen P. Hunger⁵, Mignon L. Loh⁶, Stuart S. Winter⁷, Kimberly P. Dunsmore⁸, Brent Wood⁹, Meenakshi Devidas¹⁰, Marian H. Harris¹¹, Lewis B. Silverman^{1,2}, Stephen E. Sallan^{1,2}, and Alejandro Gutierrez^{1,2,*}

¹Division of Hematology/Oncology, Boston Children's Hospital, Boston, MA 02115, USA

¹¹Department of Pathology, Boston Children's Hospital, Boston, MA 02115, USA

²Department of Pediatric Oncology, Dana-Farber Cancer Institute, Boston, MA 02215, USA

³Department of Biostatistics and Computational Biology, Dana-Farber Cancer Institute, Boston, MA 02215, USA

⁴Center for Cancer Genome Discovery, Dana-Farber Cancer Institute, Boston, MA 02215, USA

⁵Division of Oncology and the Center for Childhood Cancer Research, The Children's Hospital of Philadelphia and the Perelman School of Medicine at the University of Pennsylvania, Philadelphia, PA 19104, USA

⁶Department of Pediatrics, University of California San Francisco, San Francisco, CA 94158, USA

⁷Department of Pediatrics, University of New Mexico Health Sciences Center, Albuquerque, NM 87131, USA

⁸Division of Oncology, University of Virginia Children's Hospital, Charlottesville, VA 22903, USA

⁹Department of Laboratory Medicine, University of Washington, Seattle, WA, USA

¹⁰Department of Biostatistics, University of Florida, Gainesville, FL 32611, USA

Abstract

Users may view, print, copy, and download text and data-mine the content in such documents, for the purposes of academic research, subject always to the full Conditions of use: http://www.nature.com/authors/editorial_policies/license.html#terms

Corresponding author: Alejandro Gutierrez, Division of Hematology/Oncology, Boston Children's Hospital, 300 Longwood Avenue, Boston, MA, USA 02115, Phone: 617-919-3660; Fax: 617-730-0934, alejandro.gutierrez@childrens.harvard.edu, orcid.org/0000-0002-0249-9007.

CONFLICT OF INTEREST

The authors have no competing interests to declare.

AUTHOR CONTRIBUTIONS

M.A.B., Z.W.L., and A.G. conceived the project, designed and performed experiments, interpreted data, and wrote the manuscript. A.R.T. and M.D. performed the targeted exon sequencing and analysis. M.A.B., G.P.P., and A.G. analyzed targeted exon sequencing, RNA sequencing and array CGH data. M.A.B., E.A.S., and N.Y. performed and interpreted experiments. K.E.S. and D.S.N. performed statistical analyses and interpreted data. K.E.S., D.S.N., S.P.H., M.L.L., S.S.W., K.P.D., M.D., L.B.S., and S.E.S. aided in data collection of primary patient samples, and in analysis and interpretation of data. All authors aided in critical revision and approval of the submitted manuscript.

The role of Hedgehog signaling in normal and malignant T-cell development is controversial. Recently, Hedgehog pathway mutations have been described in T-ALL, but whether mutational activation of Hedgehog signaling drives T-cell transformation is unknown, hindering the rationale for therapeutic intervention. Here, we show that Hedgehog pathway mutations predict chemotherapy resistance in human T-ALL, and drive oncogenic transformation in a zebrafish model of the disease. We found Hedgehog pathway mutations in 16% of 109 childhood T-ALL cases, most commonly affecting its negative regulator *PTCH1*. Hedgehog mutations were associated with resistance to induction chemotherapy ($P = 0.009$). Transduction of wild-type *PTCH1* into *PTCH1*-mutant T-ALL cells induced apoptosis ($P = 0.005$), a phenotype that was reversed by downstream Hedgehog pathway activation ($P = 0.007$). Transduction of most mutant *PTCH1*, *SUFU* and *GLI* alleles into mammalian cells induced aberrant regulation of Hedgehog signaling, indicating that these mutations are pathogenic. Using a CRISPR/Cas9 system for lineage-restricted gene disruption in transgenic zebrafish, we found that *ptch1* mutations accelerated the onset of *notch1*-induced T-ALL ($P = 0.0001$), and pharmacologic Hedgehog pathway inhibition had therapeutic activity. Thus, Hedgehog-activating mutations are driver oncogenic alterations in high-risk T-ALL, providing a molecular rationale for targeted therapy in this disease.

INTRODUCTION

The Hedgehog signal transduction pathway stimulates growth and proliferation in multiple cell types during embryonic development (1–3). Loss-of-function mutations of *PTCH1*, a negative regulator of Hedgehog signaling, result in aberrant Hedgehog pathway activation, and are driver oncogenic mutations in some tumor types, including basal cell carcinoma, medulloblastoma and rhabdomyosarcoma (4–9). However, the role of Hedgehog signaling in normal and malignant T-cell development is controversial. In normal T-cell development, several lines of evidence suggest that Hedgehog signaling regulates proliferation or differentiation at multiple stages of T-cell development (10–14). However, the deletion of *Smo* in prethymic hematopoietic progenitors, which completely abolishes Hedgehog signaling, has no detectable effect on T-cell development (15, 16). Taken together, these findings suggest that acute changes in Hedgehog signaling can modulate T-cell output, but T-cell progenitors can adapt to chronic Hedgehog pathway inactivation, presumably due to compensation by alternative signals.

Hedgehog pathway mutations have recently been described in T-cell acute lymphoblastic leukemia (T-ALL) patient samples (17), and pharmacologic Hedgehog inhibitors demonstrate toxicity to T-ALL cases with autocrine Hedgehog activation (18). However, inactivating Hedgehog signaling has no effect on the onset or maintenance of *Notch1*-induced T-ALL (15), indicating that autocrine or paracrine Hedgehog signaling is not necessary for T-cell leukemogenesis. Further, despite the remarkable clinical activity of SMO inhibitors in tumors where Hedgehog-activating mutations are driver oncogenic lesions (19–22), clinical trials in tumor types with autocrine or paracrine Hedgehog activation have revealed little clinical benefit (23–26). Whether mutations that activate Hedgehog signaling drive T-cell transformation is unknown, hindering the rationale for therapeutic intervention.

Here, we report a high frequency of Hedgehog pathway mutations in T-ALL cases that are resistant to induction chemotherapy, and we show that Hedgehog signaling represses apoptosis in *PTCH1*-mutant T-ALL cells. We further demonstrate that *ptch1* mutations accelerate the onset of *notch1*-induced T-ALL in transgenic zebrafish, demonstrating that mutational Hedgehog pathway activation is a driver oncogenic lesion in the molecular pathogenesis of T-ALL.

MATERIALS AND METHODS

T-ALL clinical specimens were collected from children with newly diagnosed T-ALL enrolled on Dana-Farber Cancer Institute Study 05-001 (27), or Children's Oncology Group Study AALL0434 (28) clinical trials, with informed consent and institutional review board approval in accordance with the Declaration of Helsinki.

Complete methods are included in the SI Appendix.

RESULTS

Hedgehog pathway mutations in human T-ALL

Using targeted exon sequencing of T-ALL diagnostic clinical specimens (Supplementary Tables 1 and 2), we found 20 mutations of genes encoding canonical Hedgehog pathway components in 16% ($n = 17$ of 109) of patient samples analyzed (Figure 1a). With the exception of one case with low mutant allele frequencies (MAF) (<0.1), the MAFs (0.34–0.65) were consistent with monoallelic mutations in the bulk tumor population (Supplementary Table 1). Two of the T-ALL cases harbored monoallelic mutations of two Hedgehog pathway genes, *PTCH1*/*GLI2* and *GLI1*/*SUFU*, and a third case harbored two distinct mutations of *GLI3* at low allele frequencies. The remaining 14 T-ALL cases had a single heterozygous mutation of the pathway (Supplementary Table 1). *PTCH1* was the single most commonly mutated gene, with 9 cases harboring heterozygous missense *PTCH1* mutations (Figure 1b), all of which were validated by Sanger sequencing (Supplementary Figure 1a). Sequencing of remission specimens, which were available in 5 of the 9 cases with *PTCH1* missense mutations, revealed that 3 of these mutations were absent at remission, indicating a somatic origin, whereas 2 were detected in the remission specimen (Supplementary Figure 1b). We lacked a non-hematopoietic germline specimen to distinguish whether these were germline mutations, possibly indicating an underlying cancer predisposition syndrome, or somatic mutations associated with clonal hematopoiesis.

Hedgehog pathway mutations were associated with resistance to the initial induction cycle of intensive combination chemotherapy (Figure 1c), which suggests primary, or pre-existing, chemotherapy resistance. Hedgehog mutations were also associated with a trend towards an increased incidence of relapse or induction failure, which did not reach statistical significance (Figure 1d), but there was no difference in overall survival (Figure 1e). These findings suggest that Hedgehog-mutant T-ALL cases with a poor response to induction chemotherapy respond favorably to subsequent intensification of treatment, which is applied in response to high levels of residual leukemia. Hedgehog mutations were not significantly associated with other described biomarkers of early treatment failure, such as early T-cell

precursor (ETP) phenotype or absence of biallelic TCR γ deletion (Supplementary Figure 2), suggesting that these markers identify largely non-overlapping groups of T-ALL cases at increased risk of early treatment failure. Hedgehog pathway mutations co-occurred with a number of oncogenic lesions typical of T-ALL, such as *NOTCH1* and *PRC2* mutations, and deletions of *CDKN2A* and *TAL1* (Figure 1f and Supplementary Figure 3), although the incidence of these cooperating mutations was similar in Hedgehog-mutant versus wild-type T-ALL. These findings suggest that Hedgehog mutations can cooperate with a number of classical T-ALL oncogenic lesions in T-cell transformation.

Transduction of wild-type *PTCH1* induces apoptosis in *PTCH1*-mutant T-ALL

To investigate the role of Hedgehog signaling in T-ALL, we first focused on its negative regulator *PTCH1*, because this was the most commonly mutated Hedgehog pathway gene in this cohort. Analysis of the *PTCH1* locus in a panel of human T-ALL cell lines revealed that Jurkat cells harbored a heterozygous microdeletion of exon 2 (Figure 2a), associated with production of a mutant *PTCH1* mRNA predicted to encode a p.Gly68fsX5 truncated protein product (Figure 2b). We confirmed that this *PTCH1* p.Gly68fsX5 mutant allele was unable to silence Hedgehog signaling, as assessed by mRNA expression of the canonical Hedgehog target *Gli1*, upon transduction into ASZ001 cells derived from a *Ptch1* heterozygous knockout mouse (29, 30) (Supplementary Figure 4). In fact, expression of this mutant allele appeared to interfere with residual Ptch function in these cells. Thus, Jurkat T-ALL cells harbor a pathogenic *PTCH1* mutation.

We then asked whether transducing wild-type *PTCH1* inhibits Hedgehog signaling in *PTCH1*-mutant Jurkat cells. Transduction of wild-type *PTCH1* downregulated Hedgehog signaling, an effect that was reversed by downstream Hedgehog pathway activation using SAG, a small molecule Smoothened agonist (Figure 2c–d). Transduction of *PTCH1* impaired the viability of *PTCH1*-mutant Jurkat cells (Figure 2e), but had no toxicity to *PTCH1* wild-type CCRF-CEM or DND41 T-ALL cells (Figure 2f). Importantly, the toxicity of *PTCH1* transduction into *PTCH1*-mutant Jurkat cells was reversed by downstream Hedgehog pathway activation with SAG (Figure 2e), indicating on-target, Hedgehog-dependent toxicity. Cell cycle analysis revealed that transduction of wild-type *PTCH1* induced formation of a large sub-G1 peak, suggesting induction of apoptosis, with little effect on the cell cycle distribution of live cells (Figure 2g). To confirm that *PTCH1* transduction induced Hedgehog-dependent apoptosis in *PTCH1*-mutant T-ALL cells, we assessed effector caspase activity following transduction of *PTCH1* or *EGFP* in Jurkat cells, alone or in combination with SAG treatment. This revealed that *PTCH1* induced caspase activation, an effect that was reversed by downstream Hedgehog pathway activation using SAG (Figure 2h). Taken together, these findings demonstrate that Hedgehog signaling represses apoptosis in *PTCH1*-mutant T-ALL.

Hedgehog signaling positively regulates *MYCN* expression

The *MYCN* proto-oncogene is a transcriptional target of Hedgehog signaling in neuronal progenitors (31). *MYCN* is overexpressed in approximately 20% of human T-ALL via unknown mechanisms (32), and its overexpression drives T-cell transformation (33). Moreover, we have previously shown that overexpression of its paralog, *MYC*, represses

mitochondrial apoptosis in T-ALL (34, 35). To test whether Hedgehog signaling regulates *MYCN* transcription in T-ALL, we transduced *PTCH1*-mutant Jurkat T-ALL cells with wild-type *PTCH1* or *EGFP* control. We found that *PTCH1* transduction downregulated *MYCN* mRNA expression, an effect that was rescued by downstream Hedgehog pathway activation (Figure 2i). Analysis of *MYCN* RNA expression in the subset of primary T-ALL patient samples on which RNA sequencing was available revealed that Hedgehog mutations were associated with increased *MYCN* expression (Figure 2j), but *MYCN* RNA expression was not associated with resistance to induction chemotherapy ($P = 1.00$ by Wilcoxon rank-sum test; data not shown). These findings indicate that *MYCN* is a transcriptional target of Hedgehog signaling in human T-ALL, but suggest that other Hedgehog targets may underlie chemotherapy resistance.

Most of the identified Hedgehog pathway mutations encode pathogenic alleles

Numerous missense mutations throughout the *PTCH1* gene have been described in the cancer predisposition syndrome Gorlin syndrome (36, 37). While most of the *PTCH1* mutations we identified in T-ALL were predicted to mutate evolutionarily conserved amino acid residues (Supplementary Figure 5), none of these are known to be pathogenic. To test whether the *PTCH1* mutations identified are pathogenic, we transduced mutant alleles identified into the *PTCH1*-mutant T-ALL cell line Jurkat, and assessed their effects on leukemic cell viability and Hedgehog signaling in these cells. We found that 6 of the 7 mutant *PTCH1* alleles tested had impaired growth-suppressive activity when compared to wild-type *PTCH1* (Figure 3a), with a concordant impairment in their ability to suppress Hedgehog signaling, as assessed by *GLI1* mRNA expression (Figure 3b). Transduction of wild-type or mutant *PTCH1* alleles had no effect on the viability of *PTCH1* wild-type DND41 cells (Supplementary Figure 6). Taken together, these data indicate that most of the *PTCH1* mutations identified in T-ALL encode functionally impaired alleles.

To test whether mutations of other Hedgehog pathway genes identified induce aberrant pathway activation, we turned to NIH 3T3 cells, a mouse cell line with low basal Hedgehog activity that is competent for Hedgehog pathway activation (38). *SUFU* encodes a negative regulator of Hedgehog signaling, and transduction of NIH 3T3 cells with wild-type *SUFU* further suppressed basal Hedgehog signaling in these cells (Figure 3c). By contrast, transduction of the *SUFU* K460R mutant led to a significant increase in Hedgehog pathway activity above that in basal conditions (Figure 3c), suggesting that this allele has dominant-negative activity and can interfere with function of the wild-type protein. To test the effect of wild-type or mutant *GLI1* on Hedgehog pathway activity, we first confirmed that our RT-PCR assay for expression of endogenous mouse *Gli1* mRNA (the marker for Hedgehog pathway activation) did not cross-react with the human *GLI1* expression construct utilized (Supplementary Figure 7). Transduction of NIH 3T3 cells with the human *GLI1* G274C mutant allele did not activate Hedgehog signaling beyond the degree of activation induced by wild-type *GLI1* overexpression, suggesting that this mutation is not activating (Figure 3d). Similarly, transduction of the *GLI2* T286S mutant into NIH 3T3 cells did not activate the Hedgehog pathway beyond that induced by wild-type *GLI2* overexpression (Figure 3e). By contrast, all three *GLI3* mutant alleles identified (R292C, G1217W and R1537H) induced significantly more Hedgehog pathway activation than wild-type *GLI3*, indicating

that expression of these mutations is sufficient to induce aberrant Hedgehog pathway activation (Figure 3f). Taken together, these findings indicate that most of the Hedgehog pathway mutations identified in our T-ALL patient cohort are pathogenic. Indeed, of the 15 T-ALL cases harboring Hedgehog pathway mutations that were tested, 12 harbored mutations that were clearly pathogenic. We confirmed that the association of Hedgehog mutations with resistance to induction chemotherapy remains statistically significant if this analysis is limited to cases with known pathway activating mutations (Supplementary Figure 8; $P=0.011$).

***ptch1* mutations accelerate the onset of *notch1*-induced T-ALL**

If Hedgehog-activating mutations promote T-cell transformation in part via *MYCN* upregulation, we reasoned that this effect would be best detected in collaboration with an oncogenic lesion that promotes MYC-independent transformation. We thus turned to the zebrafish model, where *notch1a* promotes T-cell transformation without upregulating *myc* (39, 40). To generate a CRISPR/Cas9 system for lineage-restricted gene disruption, we first designed a panel of guide RNAs (gRNAs) targeting exon 13 of zebrafish *ptch1*, because mutation of this exon is known to induce aberrant Hedgehog pathway activation (41). As a control for CRISPR/Cas9-induced DNA damage, we also designed gRNAs targeting the locus syntenic to the human safe-harbor *AAVS1* locus, which is located within intron 1 of the *ppp1r12c* gene (42). To identify gRNAs that efficiently mutagenize each of these loci, individual gRNAs were co-injected with Cas9 mRNA into zebrafish embryos at the 1-cell stage, and cutting efficiency was assessed by next-generation sequencing of the target locus. This revealed gRNAs that induced insertion/deletion mutations in at least 30% of each target locus (Figure 4a). These gRNAs were then cloned into an expression vector in which the U6 promoter drives RNA polymerase III-mediated expression of the gRNA. Lineage-restricted gene disruption was achieved via a separate expression cassette within the same vector that drives expression of a Cas9-T2A-GFP self-cleaving protein under the control of the *rag2* promoter (Figure 4b, top), which drives expression in immature T-cell progenitors.

To test whether *ptch1* mutations accelerate the onset of *notch1*-induced T-ALL, we co-injected wild-type zebrafish embryos at the 1-cell stage with the CRISPR/Cas9 expression vector targeting either *ptch1* or *aavs1*, together with a *rag2* promoter-driven activated *notch1a* allele (Figure 4b). Zebrafish with successful transgene integration and expression were identified by thymic GFP fluorescence, and all fish demonstrating thymic GFP fluorescence by 4 weeks of age were screened for T-ALL onset by weekly fluorescence microscopy. Expression of the *ptch1*-targeting CRISPR/Cas9 cassette significantly accelerated the onset and increased the penetrance of *notch1*-induced T-ALL, with a median time to T-ALL onset of 13 weeks in *ptch1* fish, versus 39 weeks in the *aavs1* controls ($P=0.0001$; Figure 4c–d). Histologic analysis of leukemic zebrafish revealed diffuse infiltration of normal tissues by small cells with round to slightly irregular nuclear contours, homogeneous chromatin, and scant cytoplasm (Figure 4e), consistent with leukemic T-lymphoblasts. Next-generation sequencing of the gRNA target locus in a subset of T-ALL cases revealed the presence of dominant mutations, confirming effective mutagenesis of the intended locus and indicating a clonal origin of these leukemias (Figure 4f).

To assess the transplantability of zebrafish *ptch1*-mutant leukemias, T-ALL blasts were harvested from zebrafish with *ptch1*-mutant T-ALL, and injected into irradiated wild-type recipients (Figure 5a). We observed successful leukemic engraftment in 32 of 32 injected recipients, which rapidly progressed in all cases (Figure 5b), indicating that the aberrant growth and proliferation of these cells is cell-autonomous. Taken together, these findings demonstrate that mutational activation of Hedgehog signaling via disruption of its negative regulator *ptch1* functions as an oncogenic driver in T-ALL.

***ptch1*-mutant T-ALLs are responsive to Hedgehog pathway inhibition**

We then asked whether pharmacologic Hedgehog pathway inhibition has *in vivo* therapeutic activity in *ptch1*-mutant T-ALL. Vismodegib is a potent and specific Smoothened inhibitor with clinical activity in Hedgehog-driven human cancers (19, 43), but this drug failed to inhibit zebrafish Smoothened, as evidenced by its inability to induce cyclopia in zebrafish embryos (data not shown). Thus, we leveraged the structurally unrelated Smoothened inhibitor cyclopamine, which effectively inhibits Hedgehog signaling in the zebrafish [(44) and data not shown]. T-ALL blasts were harvested from *ptch1*-mutant or *aavs1*-control fish, and transplanted into a cohort of irradiated recipients. After T-ALL engraftment, fish were treated with either cyclopamine or vehicle control. Assessment of tumor response by fluorescence microscopy after 2 weeks of treatment revealed tumor regression in most cyclopamine-treated *ptch1*-mutant zebrafish, versus marked tumor progression in vehicle controls (Figure 5c–d, top panels). By contrast, cyclopamine had no therapeutic activity against T-ALLs expressing the *aavs1* control gRNA (Figure 5c–d, bottom panels), indicating that the effect of the *ptch1*-targeting gRNA on T-ALL is Hedgehog-dependent. Moreover, treatment of leukemic cells from patient T-ALL D15, which harbor a pathogenic PTCH1 T1106M mutation, with the FDA-approved Smoothened inhibitor vismodegib revealed that vismodegib inhibits Hedgehog signaling and impairs viability in these cells (Figure 5e). Thus, pharmacologic Hedgehog pathway inhibition has therapeutic activity against *ptch1*-mutant T-ALL.

DISCUSSION

Despite improvements achieved through the intensification of conventional cytotoxic chemotherapy, front-line therapy for T-ALL fails in 15–20% of children and 50–70% of adults (45–48), and these patients face a very poor prognosis (49–51). To date, no targeted therapies have been shown to improve clinical outcomes in this disease, highlighting the urgent clinical need for novel effective therapeutic approaches. We have identified a high frequency of Hedgehog pathway mutations in T-ALL cases with primary resistance to induction chemotherapy, and have demonstrated that mutations that activate Hedgehog signaling function as driver oncogenic events in the molecular pathogenesis of T-ALL. Given the remarkable clinical benefit of SMO inhibitors in tumors in which Hedgehog-activating mutations are driver oncogenic alterations (19–22), our findings thus provide a compelling rationale for clinical trials testing Hedgehog pathway inhibitors in patients with *PTCH1*-mutant T-ALL.

The 16% incidence of Hedgehog mutations we identified in childhood T-ALL is in line with 13% incidence reported by Dagklis and colleagues in a cohort of 67 cases of childhood and adult T-ALL (17). By contrast, a recent whole-genome sequencing (WGS) study revealed Hedgehog pathway mutations in only 4 of 264 T-ALL cases analyzed (33). One factor that likely contributed to this apparent discrepancy is the association of Hedgehog mutations with induction failure, whereas such cases appear to have been excluded from WGS analysis due to lack of a remission specimen with which to distinguish germline versus somatic variants. Additionally, accurately distinguishing missense substitutions that are pathogenic from those that are non-pathogenic passengers by informatics alone remains a major challenge, and all of the pathogenic Hedgehog mutations we identified were missense substitutions not previously known to be pathogenic. Thus, we speculate that strict algorithms for mutation calling, which are appropriately applied to WGS data to avoid the risk that the list of mutation calls will be dominated by non-pathogenic variants, may have missed pathogenic Hedgehog pathway mutations. These findings highlight the ability of functional genetics to complement genomic investigation of human disease.

Independent validation of the association of Hedgehog pathway mutations with early treatment resistance will be important before this biomarker is incorporated into clinical decision-making. Nevertheless, this finding suggests that Hedgehog signaling may directly mediate chemotherapy resistance. In acute myeloid leukemia, Hedgehog pathway activation mediates chemotherapy resistance by inducing glucuronidation of nucleoside analogs (52). Induction of apoptosis resistance provides an additional potential mechanism linking Hedgehog pathway activation to chemotherapy resistance, because mitochondrial apoptosis resistance provides one cellular mechanism for induction of resistance to conventional chemotherapy [(53–55) and unpublished observations]. However, the fact that Hedgehog mutations did not predict inferior overall survival suggests that Hedgehog-mutant T-ALLs respond favorably to the intensification of therapy applied in reaction to a poor response to induction chemotherapy. The treatment intensification strategies differed between the two clinical trials on which patients in this study were treated. On DFCI 05-001, patients with 5% leukemic blasts in the bone marrow at end-induction were deemed to have failed front-line therapy and taken off-study. While subsequent treatment was at the discretion of the treating physician, most of these patients likely underwent intensive re-induction chemotherapy followed by allogeneic hematopoietic stem cell transplantation after myeloablative doses of cyclophosphamide and total body irradiation. By contrast, on COG AALL0434, patients with 1–25% leukemic blasts at end-induction remained on study, but most were eligible for randomization to additional intensification of therapy with Nelarabine. While we remain blinded to outcomes of this randomization, it will be of considerable interest to determine whether the addition of nelarabine or allogeneic stem cell transplantation improves outcomes for patients with Hedgehog-mutant T-ALL. Even so, Hedgehog pathway inhibitors have a much more favorable toxicity profile than conventional therapy for high-risk T-ALL (19, 23, 24). Given the clear clinical activity of these drugs in tumors driven by Hedgehog-activating mutations (19–22), our findings provide a compelling rationale for clinical trials testing whether combining Hedgehog pathway inhibitors with conventional chemotherapy will improve clinical outcomes for patients with high-risk, *PTCH1*-mutant T-ALL.

Supplementary Material

Refer to Web version on PubMed Central for supplementary material.

Acknowledgments

We thank Julien Ablain for the pCS2-Cas9, pDest-Tol2-CG2-U6-gRNA, pME-MCS-zfCas9-T2A-GFP, and p3E-polyA vectors. We thank Christine Reynolds and Oscar Calzada for technical assistance; and Sofie Peirs, Bjorn Menten and Pieter Van Vlierberghe for the array CGH analysis. We thank Jessica Blackburn for the *rag2-notch1a^{ICD}* vector; and Jae Cho for the basal cell carcinoma cell line, ASZ001. We are grateful to the patients and families who provided samples for these studies. This work was supported by NIH R01 CA193651 (A.G.) and the Boston Children's Hospital Translational Research Program (A.G.). The Children's Oncology Group work was supported by U10 CA98543 (COG Chair's grant), U10 CA98413 (COG Statistical Center), U24 CA114766 (COG Specimen Banking), U10 CA 180886 (COG Operations Center), and U10 CA 180899 (COG Statistics and Data Center). M.B. is supported by the Children's Leukemia Research Association, Inc.. S.P.H. is the Jeffrey E. Perelman Distinguished Chair in the Department of Pediatrics, Children's Hospital of Philadelphia. A.G. is supported by an Investigatorship at Boston Children's Hospital.

References

1. Briscoe J, Therond PP. The mechanisms of Hedgehog signalling and its roles in development and disease. *Nature reviews Molecular cell biology*. 2013; 14(7):416–29. [PubMed: 23719536]
2. Sharpe HJ, Wang W, Hannoush RN, de Sauvage FJ. Regulation of the oncoprotein Smoothened by small molecules. *Nature chemical biology*. 2015; 11(4):246–55. [PubMed: 25785427]
3. Duman-Scheel M, Weng L, Xin S, Du W. Hedgehog regulates cell growth and proliferation by inducing Cyclin D and Cyclin E. *Nature*. 2002; 417(6886):299–304. [PubMed: 12015606]
4. Johnson RL, Rothman AL, Xie J, Goodrich LV, Bare JW, Bonifas JM, et al. Human homolog of patched, a candidate gene for the basal cell nevus syndrome. *Science*. 1996; 272(5268):1668–71. [PubMed: 8658145]
5. Hahn H, Wicking C, Zaphiropoulos PG, Gailani MR, Shanley S, Chidambaram A, et al. Mutations of the human homolog of *Drosophila* patched in the nevoid basal cell carcinoma syndrome. *Cell*. 1996; 85(6):841–51. [PubMed: 8681379]
6. Stone DM, Hynes M, Armanini M, Swanson TA, Gu Q, Johnson RL, et al. The tumour-suppressor gene patched encodes a candidate receptor for Sonic hedgehog. *Nature*. 1996; 384(6605):129–34. [PubMed: 8906787]
7. Goodrich LV, Milenkovic L, Higgins KM, Scott MP. Altered neural cell fates and medulloblastoma in mouse patched mutants. *Science*. 1997; 277(5329):1109–13. [PubMed: 9262482]
8. Hahn H, Wojnowski L, Zimmer AM, Hall J, Miller G, Zimmer A. Rhabdomyosarcomas and radiation hypersensitivity in a mouse model of Gorlin syndrome. *Nat Med*. 1998; 4(5):619–22. [PubMed: 9585239]
9. Hettmer S, Teot LA, Kozakewich H, Werger AM, Davies KJ, Fletcher CD, et al. Myogenic tumors in nevoid Basal cell carcinoma syndrome. *J Pediatr Hematol Oncol*. 2015; 37(2):147–9. [PubMed: 24517962]
10. Drakopoulou E, Outram SV, Rowbotham NJ, Ross SE, Furmanski AL, Saldana JI, et al. Non-redundant role for the transcription factor Gli1 at multiple stages of thymocyte development. *Cell Cycle*. 2010; 9(20):4144–52. [PubMed: 20935514]
11. El Andaloussi A, Graves S, Meng F, Mandal M, Mashayekhi M, Aifantis I. Hedgehog signaling controls thymocyte progenitor homeostasis and differentiation in the thymus. *Nature immunology*. 2006; 7(4):418–26. [PubMed: 16518394]
12. Furmanski AL, Saldana JI, Rowbotham NJ, Ross SE, Crompton T. Role of Hedgehog signalling at the transition from double-positive to single-positive thymocyte. *European journal of immunology*. 2012; 42(2):489–99. [PubMed: 22101858]
13. Outram SV, Hager-Theodorides AL, Shah DK, Rowbotham NJ, Drakopoulou E, Ross SE, et al. Indian hedgehog (Ihh) both promotes and restricts thymocyte differentiation. *Blood*. 2009; 113(10):2217–28. [PubMed: 19109233]

14. Rowbotham NJ, Hager-Theodorides AL, Furmanski AL, Ross SE, Outram SV, Dessens JT, et al. Sonic hedgehog negatively regulates pre-TCR-induced differentiation by a Gli2-dependent mechanism. *Blood*. 2009; 113(21):5144–56. [PubMed: 19273836]
15. Gao J, Graves S, Koch U, Liu S, Jankovic V, Buonamici S, et al. Hedgehog signaling is dispensable for adult hematopoietic stem cell function. *Cell stem cell*. 2009; 4(6):548–58. [PubMed: 19497283]
16. Hofmann I, Stover EH, Cullen DE, Mao J, Morgan KJ, Lee BH, et al. Hedgehog signaling is dispensable for adult murine hematopoietic stem cell function and hematopoiesis. *Cell stem cell*. 2009; 4(6):559–67. [PubMed: 19497284]
17. Dagklis A, Pauwels D, Lahortiga I, Geerdens E, Bittoun E, Cauwelier B, et al. Hedgehog pathway mutations in T-cell acute lymphoblastic leukemia. *Haematologica*. 2015; 100(3):e102–5. [PubMed: 25527561]
18. Dagklis A, Demeyer S, De Bie J, Radaelli E, Pauwels D, Degryse S, et al. Hedgehog pathway activation in T-cell acute lymphoblastic leukemia predicts response to SMO and GLI1 inhibitors. *Blood*. 2016; 128(23):2642–54. [PubMed: 27694322]
19. Sekulic A, Migden MR, Oro AE, Dirix L, Lewis KD, Hainsworth JD, et al. Efficacy and safety of vismodegib in advanced basal-cell carcinoma. *N Engl J Med*. 2012; 366(23):2171–9. [PubMed: 22670903]
20. Von Hoff DD, LoRusso PM, Rudin CM, Reddy JC, Yauch RL, Tibes R, et al. Inhibition of the hedgehog pathway in advanced basal-cell carcinoma. *The New England journal of medicine*. 2009; 361(12):1164–72. [PubMed: 19726763]
21. Robinson GW, Orr BA, Wu G, Gururangan S, Lin T, Qaddoumi I, et al. Vismodegib Exerts Targeted Efficacy Against Recurrent Sonic Hedgehog-Subgroup Medulloblastoma: Results From Phase II Pediatric Brain Tumor Consortium Studies PBTC-025B and PBTC-032. *J Clin Oncol*. 2015; 33(24):2646–54. [PubMed: 26169613]
22. Tang JY, Ally MS, Chanana AM, Mackay-Wiggan JM, Aszterbaum M, Lindgren JA, et al. Inhibition of the hedgehog pathway in patients with basal-cell nevus syndrome: final results from the multicentre, randomised, double-blind, placebo-controlled, phase 2 trial. *Lancet Oncol*. 2016; 17(12):1720–31. [PubMed: 27838224]
23. LoRusso PM, Rudin CM, Reddy JC, Tibes R, Weiss GJ, Borad MJ, et al. Phase I trial of hedgehog pathway inhibitor vismodegib (GDC-0449) in patients with refractory, locally advanced or metastatic solid tumors. *Clin Cancer Res*. 2011; 17(8):2502–11. [PubMed: 21300762]
24. Catenacci DV, Junttila MR, Karrison T, Bahary N, Horiba MN, Nattam SR, et al. Randomized Phase Ib/II Study of Gemcitabine Plus Placebo or Vismodegib, a Hedgehog Pathway Inhibitor, in Patients With Metastatic Pancreatic Cancer. *J Clin Oncol*. 2015; 33(36):4284–92. [PubMed: 26527777]
25. Kaye SB, Fehrenbacher L, Holloway R, Amit A, Karlan B, Slomovitz B, et al. A phase II, randomized, placebo-controlled study of vismodegib as maintenance therapy in patients with ovarian cancer in second or third complete remission. *Clin Cancer Res*. 2012; 18(23):6509–18. [PubMed: 23032746]
26. Rodon J, Tawbi HA, Thomas AL, Stoller RG, Turtchi CP, Baselga J, et al. A phase I, multicenter, open-label, first-in-human, dose-escalation study of the oral smoothened inhibitor Sonidegib (LDE225) in patients with advanced solid tumors. *Clin Cancer Res*. 2014; 20(7):1900–9. [PubMed: 24523439]
27. Place AE, Stevenson KE, Vrooman LM, Harris MH, Hunt SK, O'Brien JE, et al. Intravenous pegylated asparaginase versus intramuscular native *Escherichia coli* L-asparaginase in newly diagnosed childhood acute lymphoblastic leukaemia (DFCI 05-001): a randomised, open-label phase 3 trial. *Lancet Oncol*. 2015; 16(16):1677–90. [PubMed: 26549586]
28. Winter SS, Dunsmore KP, Devidas M, Eisenberg N, Asselin BL, Wood BL, et al. Safe integration of nelarabine into intensive chemotherapy in newly diagnosed T-cell acute lymphoblastic leukemia: Children's Oncology Group Study AALL0434. *Pediatr Blood Cancer*. 2015; 62(7):1176–83. [PubMed: 25755211]
29. So PL, Langston AW, Daniellinia N, Hebert JL, Fujimoto MA, Khaimskiy Y, et al. Long-term establishment, characterization and manipulation of cell lines from mouse basal cell carcinoma tumors. *Experimental dermatology*. 2006; 15(9):742–50. [PubMed: 16881970]

30. Aszterbaum M, Epstein J, Oro A, Douglas V, LeBoit PE, Scott MP, et al. Ultraviolet and ionizing radiation enhance the growth of BCCs and trichoblastomas in patched heterozygous knockout mice. *Nat Med.* 1999; 5(11):1285–91. [PubMed: 10545995]
31. Kenney AM, Cole MD, Rowitch DH. Nmyc upregulation by sonic hedgehog signaling promotes proliferation in developing cerebellar granule neuron precursors. *Development.* 2003; 130(1):15–28. [PubMed: 12441288]
32. Ferrando AA, Neuberg DS, Staunton J, Loh ML, Huard C, Raimondi SC, et al. Gene expression signatures define novel oncogenic pathways in T cell acute lymphoblastic leukemia. *Cancer Cell.* 2002; 1(1):75–87. [PubMed: 12086890]
33. Liu Y, Easton J, Shao Y, Maciaszek J, Wang Z, Wilkinson MR, et al. The genomic landscape of pediatric and young adult T-lineage acute lymphoblastic leukemia. *Nat Genet.* 2017
34. Gutierrez A, Grebliunaite R, Feng H, Kozakewich E, Zhu S, Guo F, et al. Pten mediates Myc oncogene dependence in a conditional zebrafish model of T cell acute lymphoblastic leukemia. *J Exp Med.* 2011; 208(8):1595–603. [PubMed: 21727187]
35. Reynolds C, Roderick JE, LaBelle JL, Bird G, Mathieu R, Bodaar K, et al. Repression of BIM mediates survival signaling by MYC and AKT in high-risk T-cell acute lymphoblastic leukemia. *Leukemia.* 2014; 28(9):1819–27. [PubMed: 24552990]
36. Lindstrom E, Shimokawa T, Toftgard R, Zaphiropoulos PG. PTCH mutations: distribution and analyses. *Hum Mutat.* 2006; 27(3):215–9. [PubMed: 16419085]
37. Stenson PD, Mort M, Ball EV, Evans K, Hayden M, Heywood S, et al. The Human Gene Mutation Database: towards a comprehensive repository of inherited mutation data for medical research, genetic diagnosis and next-generation sequencing studies. *Human genetics.* 2017; 136(6):665–77. [PubMed: 28349240]
38. Taipale J, Chen JK, Cooper MK, Wang B, Mann RK, Milenkovic L, et al. Effects of oncogenic mutations in Smoothened and Patched can be reversed by cyclopamine. *Nature.* 2000; 406(6799):1005–9. [PubMed: 10984056]
39. Chen J, Jette C, Kanki JP, Aster JC, Look AT, Griffin JD. NOTCH1-induced T-cell leukemia in transgenic zebrafish. *Leukemia.* 2007; 21(3):462–71. [PubMed: 17252014]
40. Blackburn JS, Liu S, Raiser DM, Martinez SA, Feng H, Meeker ND, et al. Notch signaling expands a pre-malignant pool of T-cell acute lymphoblastic leukemia clones without affecting leukemia-propagating cell frequency. *Leukemia.* 2012; 26(9):2069–78. [PubMed: 22538478]
41. Koudijs MJ, den Broeder MJ, Keijser A, Wienholds E, Houwing S, van Rooijen EM, et al. The zebrafish mutants dre, uki, and lep encode negative regulators of the hedgehog signaling pathway. *PLoS Genet.* 2005; 1(2):e19. [PubMed: 16121254]
42. Sadelain M, Papapetrou EP, Bushman FD. Safe harbours for the integration of new DNA in the human genome. *Nat Rev Cancer.* 2011; 12(1):51–8. [PubMed: 22129804]
43. Robarge KD, Brunton SA, Castanedo GM, Cui Y, Dina MS, Goldsmith R, et al. GDC-0449-a potent inhibitor of the hedgehog pathway. *Bioorg Med Chem Lett.* 2009; 19(19):5576–81. [PubMed: 19716296]
44. Neumann CJ, Grandel H, Gaffield W, Schulte-Merker S, Nusslein-Volhard C. Transient establishment of anteroposterior polarity in the zebrafish pectoral fin bud in the absence of sonic hedgehog activity. *Development.* 1999; 126(21):4817–26. [PubMed: 10518498]
45. Goldberg JM, Silverman LB, Levy DE, Dalton VK, Gelber RD, Lehmann L, et al. Childhood T-cell acute lymphoblastic leukemia: the Dana-Farber Cancer Institute acute lymphoblastic leukemia consortium experience. *J Clin Oncol.* 2003; 21(19):3616–22. [PubMed: 14512392]
46. Marks DI, Paietta EM, Moorman AV, Richards SM, Buck G, DeWald G, et al. T-cell acute lymphoblastic leukemia in adults: clinical features, immunophenotype, cytogenetics, and outcome from the large randomized prospective trial (UKALL XII/ECOG 2993). *Blood.* 2009; 114(25):5136–45. [PubMed: 19828704]
47. Hunger SP, Lu X, Devidas M, Camitta BM, Gaynon PS, Winick NJ, et al. Improved survival for children and adolescents with acute lymphoblastic leukemia between 1990 and 2005: a report from the children's oncology group. *J Clin Oncol.* 2012; 30(14):1663–9. [PubMed: 22412151]

48. Pui CH, Campana D, Pei D, Bowman WP, Sandlund JT, Kaste SC, et al. Treating childhood acute lymphoblastic leukemia without cranial irradiation. *N Engl J Med*. 2009; 360(26):2730–41. [PubMed: 19553647]
49. Ko RH, Ji L, Barnette P, Bostrom B, Hutchinson R, Raetz E, et al. Outcome of patients treated for relapsed or refractory acute lymphoblastic leukemia: a Therapeutic Advances in Childhood Leukemia Consortium study. *J Clin Oncol*. 2010; 28(4):648–54. [PubMed: 19841326]
50. Schrappe M, Hunger SP, Pui CH, Saha V, Gaynon PS, Baruchel A, et al. Outcomes after induction failure in childhood acute lymphoblastic leukemia. *The New England journal of medicine*. 2012; 366(15):1371–81. [PubMed: 22494120]
51. Fielding AK, Richards SM, Chopra R, Lazarus HM, Litzow MR, Buck G, et al. Outcome of 609 adults after relapse of acute lymphoblastic leukemia (ALL); an MRC UKALL12/ECOG 2993 study. *Blood*. 2007; 109(3):944–50. [PubMed: 17032921]
52. Zahreddine HA, Culjkovic-Kraljacic B, Assouline S, Gendron P, Romeo AA, Morris SJ, et al. The sonic hedgehog factor GLI1 imparts drug resistance through inducible glucuronidation. *Nature*. 2014; 511(7507):90–3. [PubMed: 24870236]
53. Vo TT, Ryan J, Carrasco R, Neuberg D, Rossi DJ, Stone RM, et al. Relative mitochondrial priming of myeloblasts and normal HSCs determines chemotherapeutic success in AML. *Cell*. 2012; 151(2):344–55. [PubMed: 23063124]
54. Bholra PD, Mar BG, Lindsley RC, Ryan JA, Hogdal LJ, Vo TT, et al. Functionally identifiable apoptosis-insensitive subpopulations determine chemoresistance in acute myeloid leukemia. *The Journal of clinical investigation*. 2016; 126(10):3827–36. [PubMed: 27599292]
55. Ni Chonghaile T, Sarosiek KA, Vo TT, Ryan JA, Tammareddi A, del Moore VG, et al. Pretreatment mitochondrial priming correlates with clinical response to cytotoxic chemotherapy. *Science*. 2011; 334(6059):1129–33. [PubMed: 22033517]

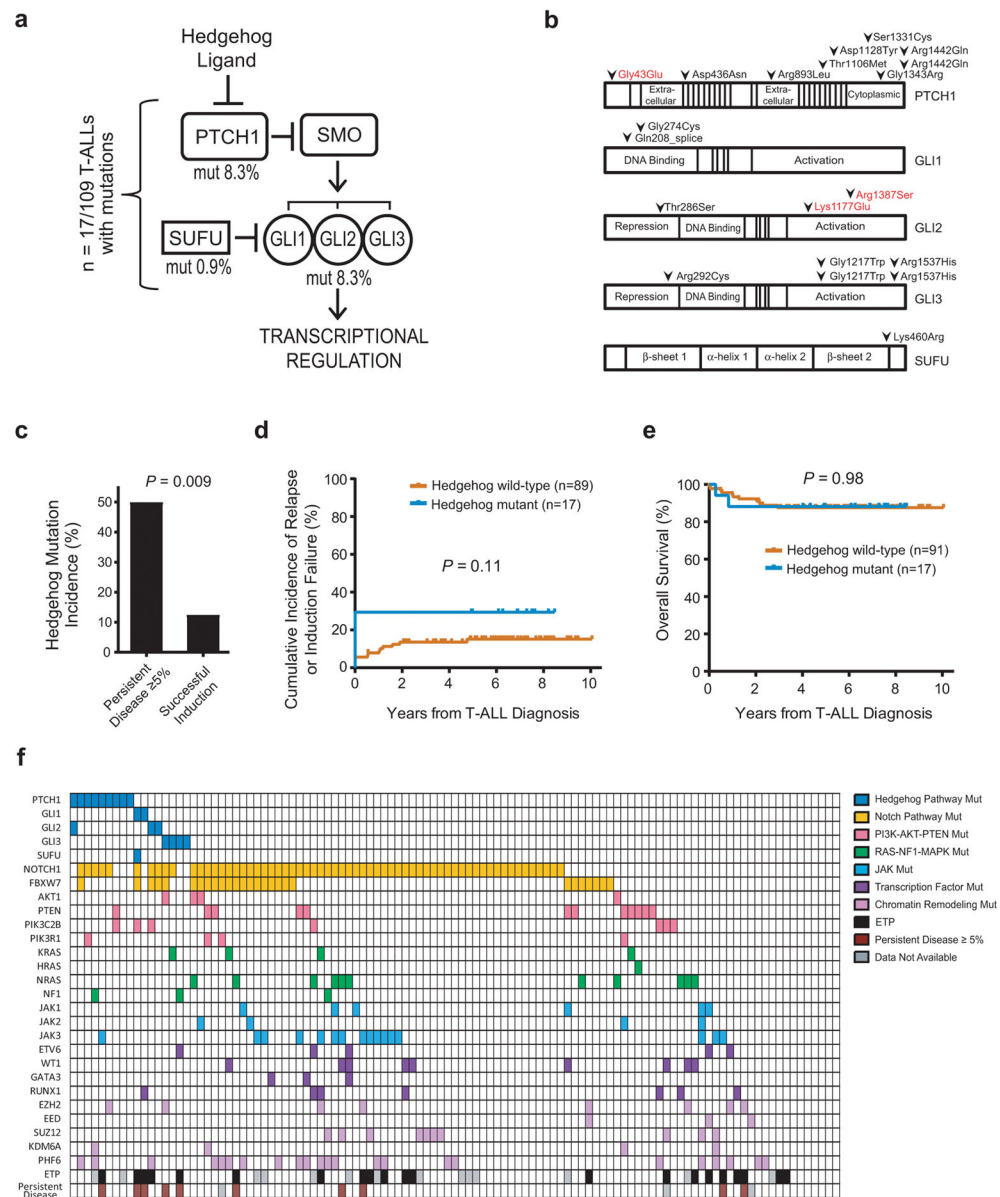


Figure 1. Hedgehog pathway mutations in childhood T-ALL

(a) Hedgehog pathway genes mutated in T-ALL. (b) Amino acid alterations predicted to result from each of the mutations identified. Amino acid numbering based on the following transcripts: *PTCH1*, NM_000264 (mutations in black font), ENST00000375274.2 (red font). *GLI1*, NM_005269. *GLI2*, NM_005270 (black), ENST00000452319.1 (red). *GLI3*, NM_000168. *SUFU*, NM_016169. Note that mutations were annotated on the transcriptional variant predicted to be most significantly affected, with detailed annotation results shown in Supplementary Table 2. (c) Association of Hedgehog pathway mutations and resistance to induction chemotherapy, defined as $\geq 5\%$ leukemic blasts in the bone marrow at end-induction by morphology (DFCI samples) or flow cytometric analysis (COG samples). Number of cases of persistent disease = 10; number of cases of successful induction = 96. A two-sided Fisher's exact test was used to assess significance. (d) Analysis

of cumulative incidence of relapse or induction failure in Hedgehog mutant (n = 17) or Hedgehog wild-type (n = 89) T-ALL patients. Note that induction deaths, which occurred in 2 Hedgehog wild-type cases, were defined as competing events in the cumulative incidence calculation. (e) Kaplan-Meier analysis of overall survival in Hedgehog mutant (n = 17) or Hedgehog wild-type (n = 91) T-ALL patients. Note that all early deaths in Hedgehog-mutant T-ALL were caused by leukemic progression. A two-sided log rank (Mantel-Cox) test was used to test for differences in survival between groups. (f) Summary of gene mutations identified in the T-ALL samples analyzed. “Persistent Disease ≥ 5%” indicates patients with induction failure or ≥ 5% end-induction minimal residual disease.

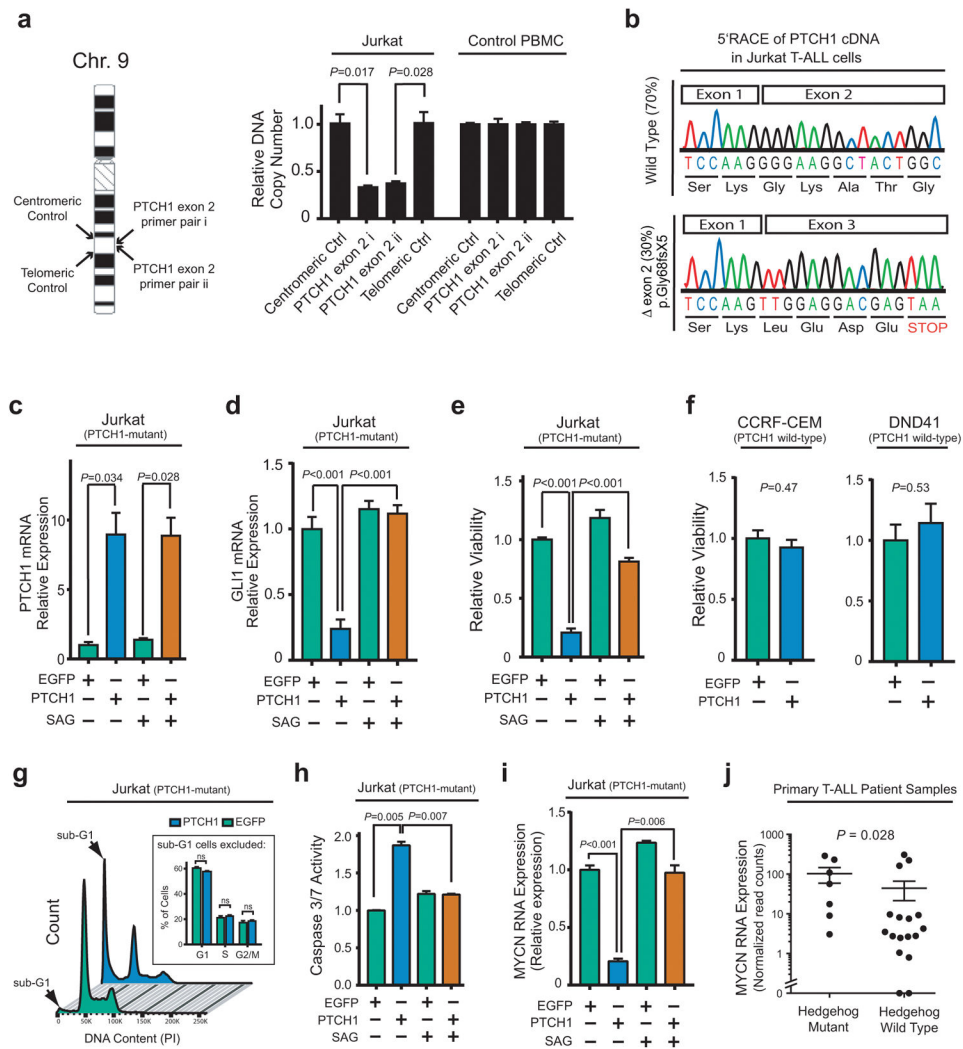


Figure 2. Aberrant hedgehog pathway activation is required for survival of PTCH1-mutant T-ALL cells

(a) Quantitative DNA PCR analysis of DNA copy number using independent primer pairs located within exon 2 of *PTCH1* (NM_000264), as well as centromeric and telomeric primer pair controls (location shown on left), on genomic DNA from Jurkat T-ALL cells. (b) 5'RACE analysis of *PTCH1* mRNA transcripts expressed in Jurkat T-ALL cells. (c–d) Jurkat cells were transduced with wild-type *PTCH1* or *EGFP* control, and treated with DMSO control or 100nM SAG to activate the Hedgehog pathway downstream of *PTCH1*. Quantitative reverse transcriptase PCR analysis was performed to assess mRNA expression of *PTCH1* (c) or *GLI1* (d), a canonical reporter of Hedgehog pathway activity. Results were normalized to β -Actin. A two-sided Welch t-test was used for statistical analysis of *PTCH1* mRNA overexpression (c), and an ANOVA with Tukey adjustment for multiple comparisons was performed to assess differences in *GLI1* mRNA expression (d). (e–f) Viability of the indicated T-ALL cells transduced with *EGFP* control or wild-type *PTCH1*, assessed 48 hours after selection in puromycin using trypan blue staining. A two-sided Welch t-test was used for statistical analysis. A Bonferroni correction was applied to adjust for multiple

hypotheses testing (e). (g) Jurkat cells transduced with *PTCH1* or *EGFP* control were harvested 48 hours after selection in puromycin and stained with PI for cell cycle analysis. A two-way ANOVA with Tukey adjustment was applied to assess differences in G1, S, and G2/M populations; p-values for each comparison in these three populations were not significant. (h) Caspase 3/7 activity in Jurkat cells transduced with *PTCH1* versus *EGFP* control, and treated with 100 nM SAG or vehicle control (DMSO); results were normalized to DMSO-treated *EGFP* control. A two-sided Welch t-test with Bonferroni correction was applied for statistical analysis. (i) Relative *MYCN* mRNA expression (normalized to β -Actin control) was assessed by RT-PCR in Jurkat cells transduced with either *EGFP* or wild-type *PTCH1*, and treated with DMSO control or 100nM SAG to activate the Hedgehog pathway downstream of *PTCH1*. A two-sided Welch t-test with Bonferroni correction was used to assess significance. (j) Association of *MYCN* mRNA expression assessed using RNA sequencing analysis in 24 of the 109 patients in this study, with Hedgehog pathway mutations. A Wilcoxon sum-rank test was used to assess significance.

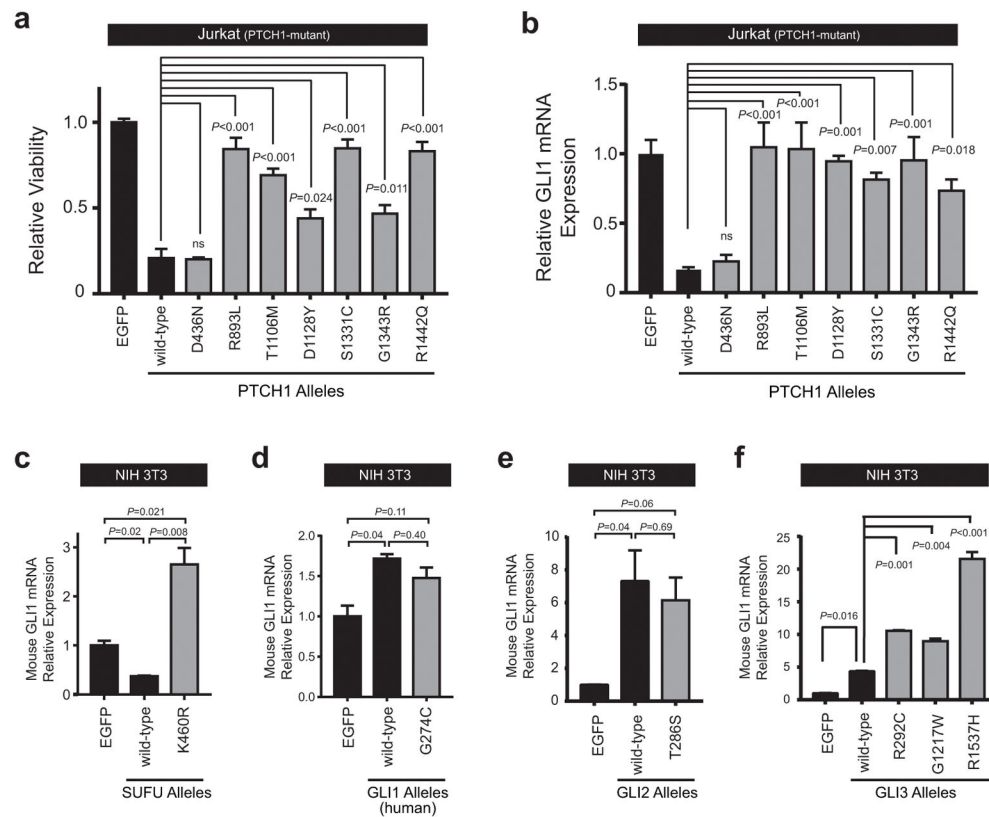


Figure 3. Most Hedgehog pathway mutations encode pathogenic alleles

(a) Jurkat cells were transduced with *EGFP* control, wild-type *PTCH1*, or *PTCH1* mutant alleles identified within our patient cohort, and viability was assessed following selection in puromycin on day 5 using trypan blue staining. Results were normalized to *EGFP* control. A two-sided, one-way ANOVA with Dunnett's adjustment for multiple comparisons was used for statistical analysis. (b) Relative *GLI1* mRNA expression (normalized to β -Actin control) was assessed in Jurkat cells transduced with *EGFP*, wild-type *PTCH1*, or mutant *PTCH1* alleles. A one-way ANOVA with Dunnett's adjustment for multiple comparisons was used for statistical analysis. NIH 3T3 mouse fibroblast cells were transfected with *EGFP* control, (c) wild-type *SUFU* or K460R mutant *SUFU* allele, (d) wild-type *GLI1* or G274C mutant *GLI1* allele, (e) wild-type *GLI2* or the T286S mutant *GLI2* allele, or (f) wild-type *GLI3*, or one of *GLI3* mutant alleles (R292C, G1217W, R1537H) identified within our T-ALL patient cohort, and relative mRNA expression of mouse *Gli1* (normalized to mouse *Gapdh* control) was assessed using RT-PCR. Results were normalized to *EGFP* control. A one-way ANOVA with Dunnett's adjustment for multiple comparisons was used for statistical analysis.

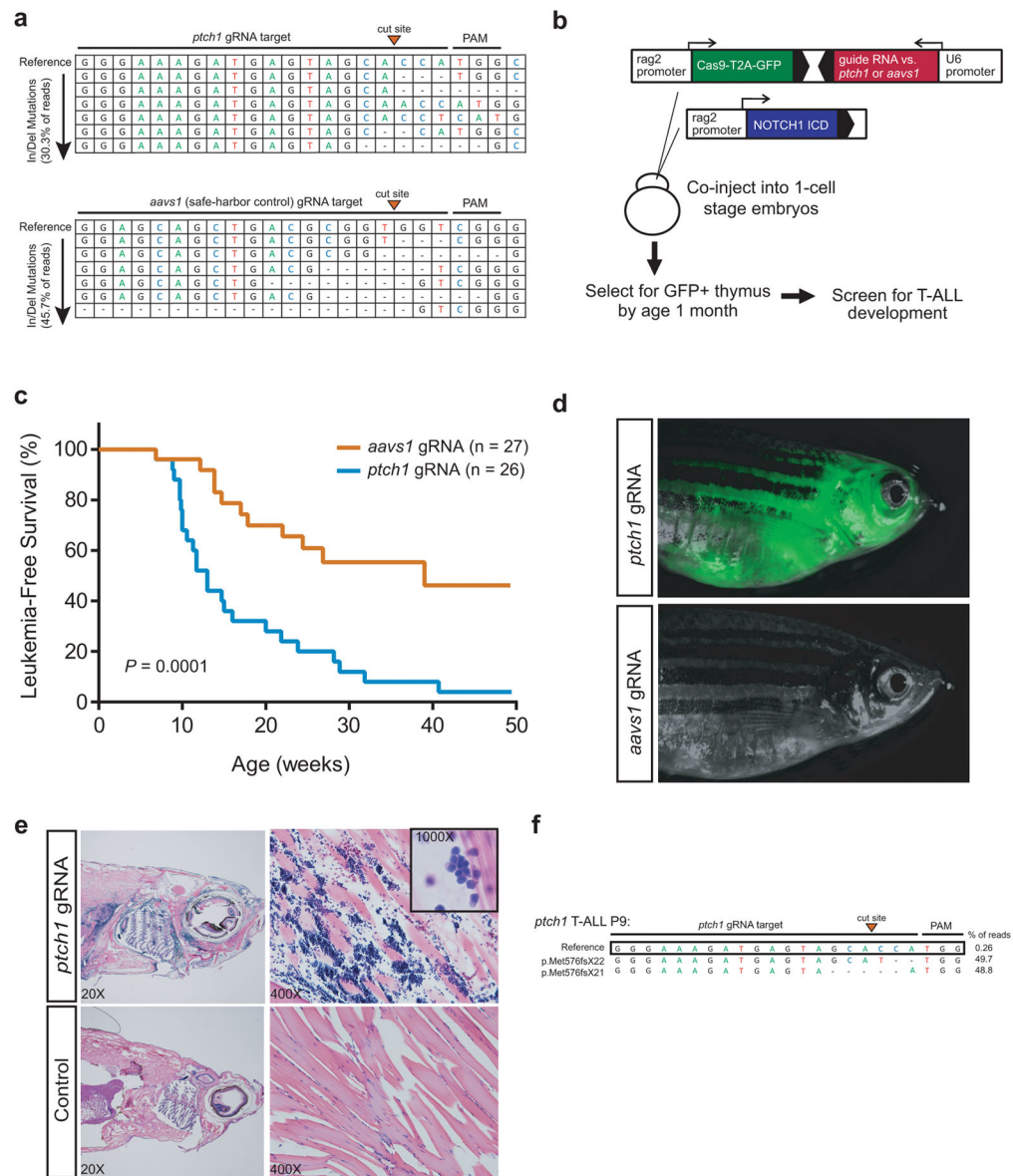


Figure 4. Mutations of *ptch1* accelerate the onset of *notch1*-induced T-ALL

(a) Guide RNAs targeting *ptch1* or the zebrafish locus syntenic to the human *aavs1* safe-harbor locus were co-injected with Cas9 mRNA into zebrafish embryos at the 1-cell stage, genomic DNA was harvested 48h later, and cutting efficiency was assessed by next-generation sequencing. Results are shown for the most efficient gRNAs targeting each locus, which were used in the subsequent generation of transgenic zebrafish. Top line indicates the reference sequence, and individual reads harboring insertion or deletion (In/Del) mutations are shown in decreasing order of abundance. The total fraction of reads with In/Del mutations is shown in parentheses. (b) Schema of experimental design. (c) Kaplan-Meier analysis of zebrafish injected with the CRISPR/Cas9 construct targeting *ptch1* or *aavs1* (safe harbor control), together with *rag2-notch1a^{ICD}* (*aavs1*, n=27; *ptch1*, n=26). A two-sided Log-rank (Mantel-Cox) test was used to assess differences in survival between these two

groups. **(d)** Representative *ptch1* (top panel) or *aavs1* (control) (bottom panel);*rag2-notch1a^{ICD}* double transgenic zebrafish at 20 weeks of age. **(e)** H&E staining of sagittal cross-section (left) and muscle (right) from *ptch1* (top) and wild-type (bottom) age-matched zebrafish. **(f)** Next-generation sequencing of the locus targeted by *ptch1* gRNA in a *ptch1*-mutant *rag2-notch1a^{ICD}* double transgenic zebrafish. Note that *ptch1* is transcribed from the strand complementary to the gRNA target sequence shown here.

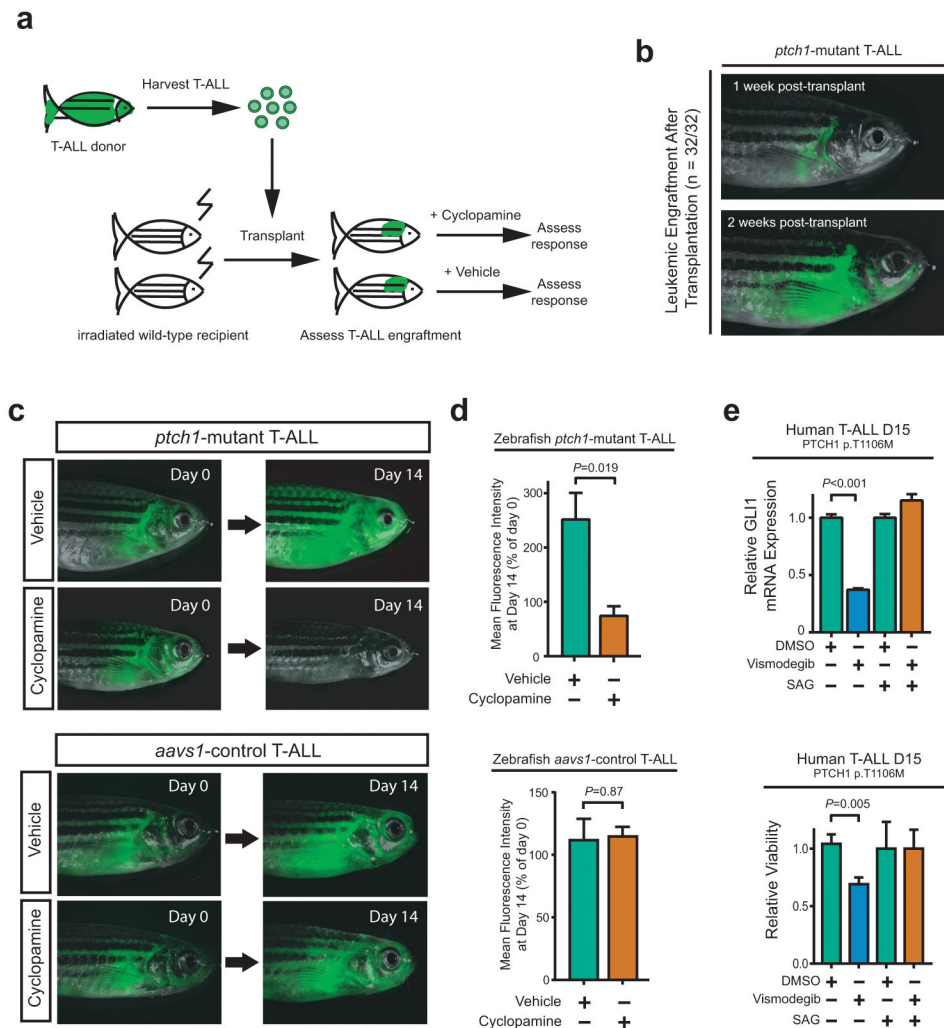


Figure 5. Transplantability of *ptch1*-mutant T-ALL and therapeutic activity of cyclopamine
(a) Schema of experimental design. **(b)** A representative adult *ptch1*-mutant recipient fish shown at day 7 (top) and 14 (bottom) following transplantation with *ptch1*; *rag2-notch1a*^{ICD} T-ALL. All 32 transplanted *ptch1*-mutant zebrafish demonstrated similar leukemic engraftment and rapid disease progression. Following leukemic engraftment, fish were treated with 1μM cyclopamine or vehicle control (ethanol) for 14 days. **(c)** Representative zebrafish in cyclopamine-treated and vehicle control (ethanol) for *ptch1*-mutant (top panel) and *aavs1*-control zebrafish (bottom panel) at the indicated time points. **(d)** Leukemic burden was assessed by mean fluorescence intensity (MFI), with MFI at day 14 normalized to day 0 for each individual fish. Of note, 5 *ptch1*-mutant fish from each group (vehicle and cyclopamine) met criteria for euthanasia due to radiation toxicity by day 14, and most others became ill soon thereafter, thus the study was terminated at this time point. A two-sided Welch t-test was used to assess differences among treatment groups. (Number of fish per group: *ptch1*-mutant recipient fish - Day 0, vehicle=10, cyclopamine=11; Day 14, vehicle=5, cyclopamine=5; *aavs1*-control recipient fish - Day 0, vehicle=9, cyclopamine=11; Day 14, vehicle=8, cyclopamine=9). **(e)** Cells from a primary T-ALL patient sample that harbored a p.T1106M PTCH1 mutation, which had been engrafted and expanded in immunodeficient

mice, were treated with DMSO control, 10nM vismodegib, or 100nM SAG. After 48 hours, (top panel) relative *GLII* mRNA expression (to β -*Actin* control) and (bottom panel) viability using trypan blue staining were assessed. Results were normalized to DMSO control. Differences were assessed using a Welch t-test.

Author Manuscript

Author Manuscript

Author Manuscript

Author Manuscript